Dear ANDI: what should I wear to be cooler in sunny and hot weather? Testing radiative performance of apparel using an outdoor thermal manikin

Faisal Abedin,[1,2**] Joseph Rotella,[1**] Shri H. Viswanathan,[1**] Cibin T. Jose,[1] Alyssa Payne,[1] Caitlyn Lyons, [1] and Konrad Rykaczewski,[1,2*]

1. School for Engineering of Matter, Transport and Energy, Arizona State University, Tempe, AZ, USA

2. Julie Ann Wrigley Global Futures Laboratory, Arizona State University, Tempe, AZ, USA

**corresponding author email: konradr@asu.edu*

***equal contribution*

Clothing properties, including color, fit, style, and textile composition, strongly influence human radiative heat gain, the dominant heat transfer pathway in hot, dry climates. Although textiles are increasingly engineered to reduce the heat load across the visible and near-infrared, and far-infrared regions, comparing realistic performance of such apparel is difficult because spectral measurements alone cannot capture interactions among the environment, clothing, and the geometry of the human body. Here, we evaluated apparel using an outdoor and internally cooled thermal manikin, "ANDI", exposed to direct sunlight under hot, low-wind conditions. By dynamically matching the manikin surface and ambient air temperatures, convective heat transfer is minimized, enabling direct measurement of net radiative heat flux. We validated the approach by comparing the outdoor performance of white and black cotton and polyester shirts under natural or controlled airflow conditions, demonstrating high repeatability at air speeds near 1 m/s. Next, we evaluated how color, fit, style, and textile composition of upper-body garments, as well as headgear, influence radiative performance. Clothing color was the dominant factor controlling radiative heat gain, with white and light-colored garments substantially outperforming dark alternatives, whereas textile composition, garment fit, and style generally had smaller effects. Similarly, light-colored hats with thicker, opaque crowns provided the greatest reduction in head heat gain, whereas black hats consisting of thin fabrics offered considerably less protection despite similar coverage. These findings reinforce long-standing recommendations to wear light-colored clothing in the sun while also demonstrating the value of objective, whole-garment testing for comparing apparel designs and validating future radiative cooling technologies intended to improve outdoor thermal comfort and safety.

Keywords: textile testing, spectral properties, radiative testing, thermal manikin

Introduction

For nearly seven decades, Americans have sought advice on personal questions through the "Dear Abby" column. However, a different kind of advisor is required when it comes to quantitative guidance on what to wear in hot, sunny conditions. Here, we show that a different kind of "columnist", the "dear" outdoor thermal manikin ANDI (Advanced Newton Dynamic Instrument), can quantitatively evaluate clothing-mediated radiative heat exchange under realistic environmental conditions. Heat exposure is a major environmental and occupational concern, especially for those spending time outdoors under direct sunlight. It ranks among the leading weather-related causes of mortality and is linked to impaired health, productivity, and occupational risk [1–6]. Clothing is one of the most accessible strategies for mitigating heat stress, but the effectiveness of recommendations such as wearing light-colored or loose-fitting garments, as well as that of many radiatively engineered textiles, remains poorly quantified due to a lack of quantitative measurement methods in real-world conditions.

In hot, sunny conditions, radiation often dominates the heat load on the human body [7–10]. Consequently, modifying the spectral properties of clothing through material and structural engineering has become a central strategy for improving outdoor thermal comfort and safety [11–14]. The spectral properties of textiles determine how fabrics absorb, reflect, transmit, and emit radiation. Significant advances have been made in tailoring fabrics to optimize these properties for upper-body apparel [15–18]. For example, fabrics have been developed with enhanced visible and near-infrared reflectance to reduce solar absorption or with transparency in the far infrared to promote thermal emission from the skin while maintaining visual opacity [18–20]. Additional approaches employ nanostructured coatings and engineered fiber assemblies to simultaneously enhance solar reflectance and mid-infrared emissivity under outdoor exposure [12, 15–17, 20–22]. However, the outdoor performance of these textiles remains poorly characterized under realistic environmental conditions.

Most studies on radiatively engineered textiles characterize spectral properties or measure temperatures and heat fluxes of flat fabric samples placed on simplified skin simulators under controlled solar exposure [12, 15–19, 21, 22]. While these approaches are useful for identifying material-level mechanisms such as solar reflection, infrared transparency, and longwave emission, they neglect the impacts of three-dimensional body and garment geometry, including air gaps, body curvature, posture, and local ventilation. They also do not fully capture the coupled radiative and convective heat-transfer processes governing clothing performance under realistic outdoor conditions (see **Fig.1**). Outdoor infrared thermography studies have demonstrated that clothing thermal behavior under solar exposure can vary substantially with environmental airflow. For example, Ichinose et al.[14] reported temperature differences exceeding 10°C between clothing colors under calm sunny conditions, with wind greatly reducing these differences. Several other studies have also evaluated the influence of clothing color on temperatures and thermal comfort under solar exposure. Early work demonstrated that black clothing increased both clothing and skin temperatures compared with white garments, even in the absence of direct solar radiation [23], while outdoor experiments consistently showed substantially higher surface temperatures for dark-colored garments than for light-colored ones [24–26]. Subsequent studies expanded these observations by relating clothing color to solar reflectance and near-infrared optical properties [27] and by modeling the coupled effects of solar absorption, conduction through clothing air layers, and external convection [28, 29]. More recently, field studies have shown that clothing reflectance and radiative cooling textiles can reduce skin temperature, improve thermal comfort, and mitigate heat strain under strong solar exposure [30–32]. However, textile temperatures do not directly translate into heat flux experienced by the person, skin temperatures vary within a small range, and thermal comfort and perception are highly subjective, making these approaches less quantitative than a heat flux measured by a thermal manikin.

Thermal manikins are widely used to evaluate the thermophysiological properties of clothing and to simulate human thermal comfort under controlled indoor conditions [11, 33–38]. There are only a few examples of outdoor manikin measurements, including using heated-only manikins seated in the shade [39], seated in a car [40], and standing while wearing protective clothing [41] in moderate conditions. Recently, a passive manikin with external anemometers and radiometers was also used to measure environmental conditions in direct sunlight [42, 43]. In our previous work, we employed the internally cooled ANDI thermal manikin, instrumented with distributed temperature and heat-flux sensors within its shell, to quantify outdoor radiative exposure under sunny, partially shaded, and fully shaded conditions (see the shell schematic in **Fig.1**) [44, 45]. By operating the manikin in isothermal mode, with the shell surface temperature maintained at the measured air temperature, we isolated the net radiative heat load by minimizing convective heat exchange between the manikin and the surrounding air. This approach enabled spatially resolved measurements of total radiative exposure and, with the addition of a white coating over portions of the shell, separate quantification of shortwave and longwave radiation loads across the body. We also conducted pilot clothing experiments using same-style, same-size long-sleeve shirts of different colors. These measurements captured not only radiative attenuation by the textiles, including transmitted solar radiation [14], but also coupled convective transport associated with elevated fabric temperatures under solar exposure (see **Fig. 1**)[45]. Under full sun and low-wind conditions, the tan torso of the manikin absorbed 159 W of radiative heat, which was reduced to 73.3 W and 86.7 W when wearing white and light-blue shirts, respectively, while darker garments produced substantially smaller reductions (e.g., to 127 W for a black shirt) [45].

Building on our prior work, the present study systematically investigates clothing-mediated radiative heat attenuation using the outdoor isothermal ANDI thermal manikin under realistic solar exposure. First, we evaluate the extent to which low-speed airflow magnitude and direction must be controlled during outdoor isothermal measurements using partial wind-isolation panels and forced airflow. Second, we use ANDI to quantify the effects of clothing color, textile type, garment fit, and garment style on radiative attenuation for commonly available torso and head garments exposed to direct sunlight. We include several types of hats because, unlike protective headgear such as helmets [46–53], the radiative attenuation provided by hats has rarely been investigated quantitatively [54–57]. Together, these experiments establish a framework for realistic evaluation of clothing-mediated radiative heat transfer and provide quantitative insight into how clothing parameters influence human radiation exposure.

Methods

Instruments

The ASU ANDI (Advanced Newton Dynamic Instrument; Thermetrics LLC, Seattle, WA, USA) is the first full-body thermal manikin specifically designed to quantify human heat exchange under outdoor extreme heat conditions. As described by Joshi et al.[44] the manikin represents a 50th percentile western adult male and consists of 35 independently controlled body segments instrumented with embedded temperature and heat-flux sensors as well as resistive heating and internal liquid-cooling channels. All supporting electronics, the water chiller, and the gas-powered generator for the manikin are mobile, allowing for outdoor experimentation. The system was operated in an approximately isothermal mode in which shell surface temperature was maintained at ambient air temperature, measured using a separate radiation-shielded sensor. Besides minor changes in how the manikin was dressed, the manikin operation was as described in our previous work [44, 45]. In particular, we did not need to cut the shirts along one arm as in our previous work, and we were able to change the shirts in under 1 minute. To provide consistent measurements, we tested on fully sunny, low-wind days (sustained wind speed of 0.25 to 1.5 m/s) in batches of 4 to 5 garments, each taking about 3 to 4 minutes for changing and reaching steady-state heat flux and temperature measurements across the covered zones. The heat fluxes and temperatures are displayed on a laptop and monitored by the operator throughout the experiment. The manikin position was adjusted approximately every 10 minutes based on matching symmetric shadows from two sides of the supporting stand, resulting in it nearly continually facing the sun directly (see **Fig.2A**). In addition to ANDI, we also utilized the advanced biometeorological station MaRTy, which measures shortwave and longwave radiation in cardinal, downward, and upward-facing directions, air temperature, humidity, and wind speed (see Middel et al. for detailed instrument description [58]). The cart is used to obtain high-end radiatively shielded air temperature measurements to guide ANDI shell temperature adjustment and wind speed measurements to avoid excessively gusty periods. We also used MaRTy's radiative measurements to benchmark the total net radiative heat flux measured by the "nude" manikin, based on calculations developed by Joshi et al. and Sadeghi et al. [44, 45].

For testing clothing performance, we typically conducted three repetitions of each garment set, ensuring that garment air gaps and fit were kept as consistent as possible when changing sizes and styles. In the reported data, we did not apply any corrections or normalization methods for solar zenith angle variation. The heat flux sensor consists of two custom-made, calibrated resistive temperature sensors, each with an uncertainty of approximately 0.05 °C distributed over its respective zone area. The sensors are separated by a thin layer with known thermal conductance. Based on error propagation, the theoretical uncertainty in heat flux is ±13 W/m^2, with zone-to-zone variations of approximately 1 W/m^2. The measurement uncertainty was also quantified experimentally by the manufacturer by calibrating the heat flux sensor against heat generated by the resistive heater integrated into the manikin shell. Across a wide range of heat flux values, approximately 75 to 500 W/m^2, the experimentally determined uncertainty was generally lower than the theoretical value, not exceeding 5% of the measured value and averaging below 2% across all zones. For example, in the zone where the lowest reported measurements were obtained, the top of the head, the experimentally quantified uncertainty was only 1.5% at 145 W/m^2. However, for near-vanishing heat fluxes below 25 W/m^2, the measured values approach twice, or less, the theoretical uncertainty. With the convective component eliminated, the nude manikin radiative outdoor experiments are independent of wind gusts and very stable, gradually changing with solar angles and surrounding surface temperatures [44, 45]. Therefore, as previously [44, 45], for heat fluxes measured with the nude manikin, we report a conservative fixed ±13 W/m^2 uncertainty.

In our previous and current experiments with a clothed manikin, we found that adding clothing increased the variation between repeated experiments beyond the instrumental uncertainty, indicating that repeatability was primarily limited by airspeed variability. However, these differences remained well within ±15% (80% confidence interval) at airspeeds below 1.5 m/s. Although we monitored wind speed and avoided measurements during gusts exceeding 1.5 m/s, we chose to adopt a conservative combined uncertainty of ±15% (80% confidence interval) for all reported experimental values to account for the possibility that the effects of outdoor airflow variability could be greater under environmental conditions encountered on other measurement days. Statistical significance for pairwise comparisons between experimental conditions, garment parameters (color, size, style, fiber type), and testing configurations was evaluated using a two-sided inverse-variance Z-test on measured net heat flux and integrated heat rate values. Two-tailed p-values were calculated for key pairwise contrasts, with statistical significance defined at $p<0.05$.

To calculate the total net radiative heat rate (unit: Watts) for the entire garment-covered area of the manikin, we summed the products of the measured net radiative heat fluxes with corresponding zonal areas (face: 0.039 m^2, head: 0.0455 m^2, neck: 0.0529 m^2, chest: 0.086 m^2, stomach: 0.077 m^2, underarm: 0.031

m^2, upper arm front: 0.0529 m^2, upper arm back: 0.0327 m^2, forearm front: 0.0452 m^2, forearm back: 0.0269 m^2, shoulder: 0.0171 m^2, upper back 0.0781 m^2, lower back 0.0584 m^2).

Field Experiments

We conducted measurements on an unobstructed site on the roof of the Novus parking garage in Tempe, Arizona (33.422°N, 111.928°W, 373 m elevation) on four cloudless days (March 19th, 25th and 26th, and April 20th of 2026). The experiments were conducted starting shortly before noon and lasting 4 to 5 hours, with air temperatures ranging from 33.6°C to 42.6°C, dew points of 1.11°C to 3.33°C, and solar zenith angles from 33.7° to 77.8°. We selected the afternoons to conduct the experiments because the air temperature is stable, with changes on the order of 0.5 to 1°C per hour, reducing the need to adjust manikin shell temperature setpoints.

Semi-outdoor wind tunnel

The semi-outdoor configuration enabled controlled airflow measurements while maintaining realistic rooftop radiative exposure conditions (see **Fig.2B** and **2C**). It was constructed with 15 mm aluminum T-slot extrusions and 1.22x2.44 m(4x8ft) Styrofoam panels. The interior side of the panels was spray-painted black (shortwave and longwave absorptivity of 0.95) to provide consistent side conditions and prevent any reflections, while the outside was covered with a reflective aluminum coating to minimize unwanted radiative heating. The two panels were connected in a parallel configuration with 1.27 m of space between them, matching the typical indoor wind tunnel width (see **Fig. 2B-D**) [59]. The panels were raised 2.54 cm from the ground. ANDI was placed in the center of the structure, with its feet being raised about 25.4 cm from the ground. To impose a low-speed about 0.5 m/s airflow directly over the torso area of the manikin, a 0.61 m (24″) diameter fan (Xpower FD-630D) with continuous velocity adjustment was placed on a stand about 1.5 m in front of the manikin. The air flow velocity was measured at 20 Hz using a 3D ultrasonic anemometer (CSAT3B, Campbell Scientific), also allowing for calculation of turbulence intensity and turbulence length scales. At the same time, MaRTy was placed 2 m behind ANDI and was used to measure the “background” outdoor airflow using its ultrasonic anemometer. The entire enclosure was mobile and taken to the outdoor measurement site with each experiment.

Materials

Fig. 3 shows the 20 shirts and 9 hats that we tested using the manikin in this study. The long sleeve **A.** black 100% polyester (Nike, FB7070-010, Men’s, size: US-L), **B.** black 100% cotton (H&M, On/ 502236, regular fit, Men’s US-L), **C.** white 100% polyester (Nike, FB7070-010, Men’s, size: US-L), and **D.** white 100% cotton (H&M, N 437432, regular fit, Men’s, US-L) shirts were used in studies comparing measurement setups (unobstructed, in a semi-wind tunnel with and without a fan). To assess impact of style and color, we also measured the **E.** tan 100% polyester T-shirt (Sport-Tek, ST350, Men's, L), **F.** white and **G.** tan 100% recycled polyester "hiking" shirts (Ozark Trail, OT13750L, Men's, L), and **H.** combat shirt with sleeves made of 50% nylon and 50% cotton and torso made of 100% polyester with moisture-wicking and antimicrobial treatment (Propper OCP, Men's, L), **I.** Air Force OCP Hot Weather Uniform Coat made from Cordura Nyco fabric (Tru-Spec, Men's, L) and **J.** "construction" assembly (the tan T-shirt, generic high visibility yellow mesh polyester vest, with white reflective sleeves on forearms). To test the impact of long-sleeve shirt size, we purchased a set of **K.** white and **L.** black 100% cotton shirts with sizes S, M, L, XL, and XXL (Eklentson Men's Crewneck, EK-600-L23M949D, varied sizes).

The tested head gear included wide-rim **M.** tan sun straw hat made of 80% paper and 20% polyester (Trifabricy, TYDYCMKQ115CM9L, Floppy Foldable Summer Hat, Women's, One Size), **N.** tan light thin made of 100% polyester (Mission, Cooling Boonie Hat, Unisex, One Size), and **O.** tan Tilley hat made of 36% polyester, 29% hemp, 28% cotton, and 7% rayon (Tilley, TMH55, Airflo Mashup Sand, Unisex, 7.5), as well as **P.** light tan baseball cap made of 100% cotton (Furtalk, B0BZNR7S6V, unisex, Medium-Large), **Q.** light tan visor (open head) made of 100% cotton (Andiceqy, B0D9DNB3S3, Sports Sun Visor, Unisex) and **R**. black, **S.** dark gray, **T.** light gray and **U.** tan "bucket" 100% cotton hats (PFFY Bucket Hat, B09XHKFLNN, One size).

Spectroscopic characterization of selected textiles

The spectroscopic performance of the samples was evaluated using two instruments: a PerkinElmer Lambda 950+ UV/VIS/NIR Wide Band Spectrometer and a PerkinElmer Frontier FTIR spectrometer. For the UV/VIS/NIR measurements, the cut region of each sample was aligned with the instrument's beam path, and reflectance spectra were collected over the wavelength range of 0.25–2.5 μm. The acquired spectra were then processed using DPV software integrated with UV WinLab to extract the relevant data. Long-wavelength spectroscopic characterization was performed using the PerkinElmer Frontier FTIR equipped with a DiffusIR accessory. Samples with a diameter of 0.5 inches were measured over the 2.5–25 μm wavelength range. FTIR spectra were collected to compare the reflectance of the mirror samples with that of the background. The fractional spectral reflectivity plots are shown in Appendix 1, while the solar and far-infrared region reflectivities were calculated by integrating and scaling the product of the spectral reflectivity with corresponding blackbody emissivity distributions [45].

Results

Measurement of radiative textile properties does not require control of airflow on low wind days

The semi-outdoor wind tunnel and fan successfully imparted adjusted airflow on ANDI, however, our results show that this setup is unnecessary for radiative textile testing in low-wind conditions. Tests conducted with anemometers placed inside and outside of the semi-outdoor wind tunnel walls revealed a substantial reduction in wind direction variance, with a concentration of wind angles parallel to the tunnel walls within the enclosure (see wind direction plots in **Fig.4**). Throughout the test, the ambient wind speed was 1.03±0.6 m/s (±1 standard deviation). With the fan at the lowest setting, wind speeds inside the enclosure were reduced to 0.64±0.09 m/s. With the fan on, we were able to adjust the continuous power input setting to achieve a consistent 0.9±0.07 m/s in a direction parallel to the enclosure.

Fig. 4 A-C shows results of measurements with ANDI wearing the white and black polyester and cotton long sleeve shirts with the three outdoor testing setups illustrated in **Fig.2**. The white and black shirts made of the two fabrics have comparable solar range reflectivity (0.67 for white and 0.33 for black single layer of polyester and 0.71 for white and 0.30 for black single layer cotton, see Appendix 1 for the spectral reflectivity distributions). For the nude manikin, the measured net heat flux was highest on the most sun-exposed zones, including the stomach and chest (394±13 to 445±13 W/m^2 for the latter), and lowest on the back (near 0 W/m^2). All textiles reduced measured net heat flux compared to the nude condition. The white shirts showed the greatest reduction relative to the nude condition (for the chest zone, 187±28 to 216±32 W/m^2), while black shirts had cooling levels between the white and nude conditions (for the chest zone, in the range of 342±51 to 407±61 W/m^2).

The textile material generally had a minor effect on the net heat flux when compared with the dominant influence of color. At most, with ANDI in the open (no enclosure or fan), the black cotton shirt resulted in a measured heat flux on the chest of 342±51 W/m^2 while the black polyester shirt was 361±54 W/m^2. This 5% difference is below the typical experimental uncertainty and was not statistically significant according to a two-sided inverse-variance Z-test ($p=0.744$). In contrast, changing from a black cotton to a white cotton shirt (187±28 W/m^2) under identical conditions produced a statistically significant reduction in chest heat flux ($p<0.001$).

In general, **Fig. 3D** shows that, despite significant changes in airflow directionality with and without the enclosure, the difference in the measured net heat flux among the three outdoor testing methods across all fabric types and colors is negligible. Even the largest observed differences between measurement setups for the same textile and color, such as for white polyester shirt with the manikin in the open (178±28 W/m^2) and standing in enclosure with fan on (216±32 W/m^2) and for black polyester shirt with the manikin in the open (361±54 W/m^2) and standing in enclosure with fan off (407±61 W/m^2), are not statistically significant ($p=0.245$ and $p=0.469$, respectfully). The close match in zonal heat flux measurements also translated to close heat rate measurements integrated across the textile-covered areas. For example, there are no statistically significant differences between total heat rates across the covered upper body for the black polyester shirt, which were 93.7±15 W for the no-enclosure case, 106±16 W for the enclosure-and-no-fan case, and 99.3±15 W for the enclosure-and-fan case (for 93.7±15 W vs. 106±16 W, p=0.457). Following these results, the remaining outdoor tests were conducted without the semi-outdoor wind tunnel and fan.

Size of the long sleeve shirt has a minor impact on radiative heat flux

Fig. 5 shows there is no consistent correlation between shirt size and the measured radiative net heat flux. While larger white shirts showed a slight numeric increase in stomach and chest heat fluxes (e.g., 139±21 W/m^2 for the S size vs. 175±26 W/m^2 for the XXL size on the chest, see **Fig. 5A**), this difference was not statistically significant (p=0.168). Similarly, the difference between S and XXL black shirts across the chest zone (318±48 W/m^2 vs. 350±52 W/m^2, see **Fig. 5B**) was not statistically significant (p=0.563). In contrast, an increase in the size of the black shirts led to a statistically significant reduction in radiative heat in the arm zones. The front forearm zone provides the most notable example, with the S and XXL shirt net heat fluxes measuring 236±35 W/m^2 and 153±23 W/m^2, respectively (p=0.011). However, these local differences had no statistically significant impact on the total heat rate values across the textile-covered areas. For example, the covered upper-body heat rates for the black long-sleeve shirts with sizes S, M, L, XL, and XXL were 103±15, 95.1±14, 92.5±14, 89.7±13, and 86.9±13 W, respectively (p=0.278 for S and XXL pairwise comparison). For white shirts, these values were 44.3±7, 44.6±7, 48.0±7, 50.3±7, and 55.4±8 W (p=0.181 for S and XXL pairwise comparison). Therefore, we proceeded to measure the impact of shirt style using L-sized shirts.

Shirt style has a weaker effect than its color on radiative heat flux

Fig. 6 shows the results of upper-body radiative heat flux measurements for ANDI wearing various styles and colors of upper-body garments, from plain long-sleeve shirts to military and construction-like outfits. In the most sun-exposed zones, such as the chest and stomach, garment style had a significantly weaker effect on radiative heat flux than garment color. A pairwise contrast between plain black and plain white long-sleeve polyester shirts showed a major difference (349±52 W/m^2 vs. 186±28 W/m^2, p=0.0004). By comparison, changes in shirt style within the same color family showed a minor difference that was not statistically significant. For example, in the chest zone, there is no statistically significant difference between the heat fluxes measured with the white polyester plain long-sleeve and hiking shirts (186±28 W/m^2 vs. 152±23 W/m^2, p=0.226), between light tan polyester hiking and short-sleeved shirts (203±30 W/m^2 vs. 252±38 W/m^2, p=0.196), or between the army camo and hot weather gear (224±34 W/m^2 vs. 279±42 W/m^2, p=0.188).

In other zones, both army outfits (army hot weather and army camo) resulted in net radiative heat fluxes close to that of the black polyester shirt, particularly for the stomach, shoulder, and upper arm zones. The front upper arm zone provides the best example of this, with black polyester, army hot weather, and army camo having basically identical heat fluxes of 138±21, 140±21, and 138±21 W/m^2 ($p=0.93$), respectively. An interesting outlier measurement was due to the "construction" outfit, which provided a dramatic drop in measured net radiative heat flux across nearly every zone. One of the largest drops is seen in the stomach zone, where the tan shirt yielded a heat flux of 157±24 W/m^2, while the full worker's outfit, including the reflective yellow vest over the shirt, was just 52±8 W/m^2 (157±24 W/m^2 vs. 52±8 W/m2, $p<0.001$). The fact that this value is about three times lower than other stomach measurements with light colored shirts likely stems from the combination of the highly reflective stripes covering most of the stomach and the effective radiation "shielding" provided by two layers of garments. In total terms, wearing the shirts reduced the heat rate for the torso and upper arms from 125±19 W (nude) to 92.9±14 W (black polyester), 52.4±8 W (white polyester), 54.5±8 W (white hiking), 62.3±9 W (tan hiking), 84.3±13 W (tan short-sleeve), 56.1±8 W (construction outfit), 87.3±13 W (hot weather army coat), and 77.5±12 W (army combat shirt).

Light-colored, thicker fabric hats reduce radiative heat flux on the head

Fig. 7A compares radiative heat fluxes measured on the three head zones, including "head" (i.e., top of the head), the face, and the "neck" that includes the back of the head (the zones are indicated in images of ANDI in **Fig.7B**). The hats are predominantly in physical contact with the head zone and small parts of the other two. Accordingly, the reduction in heat flux measured on the face and neck is primarily due to shading. As with the shirts, wearing any hat reduces the measured radiative heat fluxes on zones directly exposed to the sun (head and face), but, interestingly, can moderately increase the heat flux on the neck zone above the nude baseline. This effect likely stems from solar heating of the hat material and direct conductive heat flux on the zone. The head, or more accurately the head top zone, is most completely covered by the hats, therefore most relevant to discuss. As in the case of the shirts, the hat color provides the strongest correlation with the measured radiative heat flux. In particular, the nearly white, light-tan baseball cap dramatically reduces the baseline "nude" heat flux of 190±28 W/m^2 to 34±13 W/m^2 ($p<0.001$), while a black bucket-type hat only reduces it to 118±18 W/m^2 (190±28 W/m^2 vs. 118±18 W/m^2, $p=0.0059$). In fact, the reduction in heat flux provided by the black bucket hat is so low that it is equal to the 118±18 W/m^2 heat flux measured with the "tennis hat" visor that has an open, sun-exposed top ($p=1$). Another surprising observation is that putting on the tan and thin polyester sun hat on the manikin resulted in a heat flux of 101±15 W/m^2 that is not statistically different from the black bucket hat heat flux (101±15 W/m^2 vs. 118±18 W/m^2, $p=0.349$), but also a much higher heat flux than a similarly tan-colored but thicker top "airflo" sun hat (58±9 W/m^2 vs. 118±18 W/m^2, $p<0.001$), or similarly cream-colored bucket hat (56±9 W/m^2 vs. 118±18 W/m^2, $p<0.001$) and the tan straw hat (48±7 W/m^2 vs. 118±18 W/m^2, $p<0.001$). Changing the bucket hats to light gray and gray only increased the head heat flux slightly, to 68±10 and 70±10 W/m^2, respectively. We discuss the observed trends in shirt and hat heat fluxes in the next Section.

Discussion

Outdoor testing: unobstructed and partially-wind obstructed configurations

The unobstructed outdoor and semi-outdoor measurements produced similar heat transfer trends for white and black long sleeve shirts, despite differences in local airflow direction variability. This indicates that radiative load dominated the net clothing heat gain under the tested environmental conditions. Black garments absorbed substantially more shortwave radiation, increasing clothing surface temperature and enhancing convective cooling. However, the magnitude of the convective contribution remained relatively small compared with the absorbed radiative heat flux. In particular, for the chest region, typical convection coefficients for 1 m/s wind speed are about 9 W/m^{2}K [60] and clothing surface temperature differences in the range of 2 to 10°C [14] result in convective heat transfer of 20 to 90 W/m^2. In contrast, for dark garments that heat up by 10°C above ambient air temperature due to absorbed radiation, the net heat gain is on the order of 300 to 500 W/m^2. Since the convective heat transfer coefficients scale with about the square root of the wind velocity, there is a minor difference in convective heat transfer between 1 and 1.5 m/s. For example, employing de Dear's correlation for the chest heat transfer coefficient ($9.1v_{air}^{0.59}$ [60]), increasing the wind speed from 1 to 1.5 m/s leads to a minor change in the heat transfer coefficient from about 9 to 11 W/m^{2}K. This comparison of convective and radiative heat fluxes from the shirts with equal air and manikin shell temperatures explains why moderate variations in outdoor airflow at low air speeds, around 1 m/s, are not expected to substantially alter the relative clothing performance trends observed between the unobstructed and semi-outdoor configurations. We note that Ichinose et al. [14] observed that the temperature difference between white and black shirts began to diminish at air speeds around 3 m/s. Accordingly, care should be taken to conduct outdoor radiative textile testing using the thermal manikin at low (~1 m/s) air speeds, while measuring wind speed and avoiding measurements during wind gusts.

ANDI's (radiative) cool shirt and hat recommendations

To reduce heat gained through radiation in hot, low-wind conditions outdoors, our ANDI experiments show that wearing light-colored clothing provides substantial benefits, while the textile (cotton vs. polyester), garment style, and size have only minor effects. Consistent with our prior results [45], changing from a black to a white shirt reduces the maximum radiative heat flux (on the chest) by about 50%, or by 200 W/m^2 when the nude measurement was around 450 W/m^2. In terms of total heat rate absorbed by the shirt-covered torso, this translates to a reduction in net radiative heat gain of about 30-50 W, with the exact amount depending on solar and infrared irradiation. To put it in perspective, a typical adult male generates about 100 W (1 MET) at rest; therefore, choosing a light rather than a dark long-sleeve shirt can reduce the body's heat load by about one-third to one-half. Such a reduction in maximum local heat gain on the main, large, sun-exposed area, such as the chest in our experiments, will yield major reductions in local skin temperature and thermal comfort benefits. In turn, even a one-third-to-half-MET reduction in overall heat gain can improve thermal safety for both individuals who are stationary during prolonged sun exposure and those performing strenuous activity (e.g., agricultural work [61]). Lastly, the observation that the yellow vest with highly reflective elements produced the lowest radiative heat flux on the stomach region motivates the use of our methodology to evaluate the radiative attenuation performance of novel radiatively engineered textiles in the future.

While most of the radiative heat flux attenuation provided by hats can be related to their color or zone coverage, our observation that hats with thinner tops provide worse outcomes is more surprising. To start with, wearing any hat reduces the heat absorbed by the head, but wearing a black one is a poor thermal choice as it provides the same top-of-the-head radiative heat flux as wearing a visor with mostly open top. For similarly light-tan and tan colored hats, the thickness of the fabric covering the top of the head strongly influences the radiative heat flux. In particular, the 0.19 mm thin polyester hat resulted in a head heat flux of 101±15 W/m^2 that is much higher than the one measured for the 1.44 mm thick airflo hat (58±9 W/m^2), the 0.59 mm thick baseball cap (34±5 W/m^2), the 1.51 mm thick straw hat (48±7 W/m^2), or the 0.74 mm thick bucket hat (56±8 W/m^2). Therefore, while the comparison is not exact because the colors do not match perfectly, a major increase in radiative heat flux occurs as the top hat layer decreases from about 0.6 to 0.2 mm. Physically, this effect likely stems from the thicker fabric providing at least threefold higher thermal resistance to the transfer of solar heat absorbed on the exterior hat surface to the manikin head (0.015 vs. 0.005 m^2°C/W with assumed thermal resistance of 0.04 W/m°C [62]). Alternatively, the thinner fabric might be slightly transparent, whereas the opaque, thicker hats fully block direct solar exposure.

Limitations and future improvements

While this work focused on quantifying the radiative attenuation provided by various clothing items under realistic outdoor conditions, it is important to emphasize that human thermal comfort and heat stress are governed by the net heat flux at the skin resulting from multiple simultaneous heat transfer pathways. The isothermal experimental methodology was intentionally designed to suppress convective heat transfer and exclude sweat evaporation, thereby isolating and quantifying the contribution of dry radiative heat flux. Consequently, the reported measurements should not be interpreted as representing the overall thermal performance of clothing during actual wear.

In hot environments, cooling via sweat evaporation is the primary physiological mechanism for heat dissipation [63–66]. Therefore, clothing that provides high solar reflectance or radiative shielding should also maintain high water vapor permeability to avoid impairing sweat evaporation. These characteristics should be evaluated both independently, to understand the influence of individual textile design parameters, and together, to assess the overall cooling performance of garments under realistic wearing conditions. Building on the current contribution, future studies should address the following research directions:

- Sweating-manikin measurements under outdoor conditions, or equivalently within a climate-controlled chamber equipped with a validated large-scale solar simulator and wind enclosure, to quantify the combined effects of radiation, convection, and sweat evaporation.
- Assessment of additional human postures and activities, such as walking and sitting, to determine how changes in body orientation and motion influence solar exposure and garment performance.
- Evaluation of radiatively engineered textiles, including fabrics specifically designed to maximize solar reflection while maintaining high moisture vapor permeability, to assess the trade-off between radiative protection and evaporative cooling.
- Investigation of hair effects on hat performance [67, 68], recognizing that hair properties introduce additional variables that may require longer-duration or more controlled experiments than the present quasi-steady outdoor methodology.

Conclusions

We demonstrated that the outdoor ASU ANDI thermal manikin operating in an approximately isothermal mode with air provides a practical and quantitative approach for evaluating clothing-mediated radiative heat transfer under realistic environmental conditions. By minimizing convective contributions and directly measuring body-segment heat fluxes under natural solar irradiation, the method captures the combined effects of textile optical properties, garment, and body shape that are difficult to reproduce using flat fabric tests or indoor solar simulators. The finding that unobstructed outdoor measurements yield results comparable to those under partially controlled airflow conditions further simplifies the experimental methodology and supports its use as a standardized platform for evaluating conventional and emerging radiatively engineered textiles.

Beyond establishing a measurement framework, our experiments provide quantitative guidance for clothing selection in hot, sunny environments. Clothing color was the dominant factor controlling radiative heat gain, with white and light-colored garments substantially outperforming dark alternatives, whereas textile composition, garment fit, and style generally had smaller or no effects. Similarly, light-colored hats with thicker, opaque crowns provided the greatest reduction in head heat gain, whereas black hats and thin fabrics offered considerably less head protection despite similar coverage. These findings reinforce long-standing recommendations to wear light-colored clothing in the sun while also demonstrating the value of objective, whole-garment testing for comparing apparel designs and validating future radiative cooling technologies intended to improve outdoor thermal comfort and safety.

Acknowledgments

Authors gratefully acknowledge the use of spectroscopy equipment within the Eyring Center for Solid State Science at Arizona State University.

References

[1] Arbuthnott KG, Hajat S. The health effects of hotter summers and heat waves in the population of the United Kingdom: A review of the evidence. *Environmental Health: A Global Access Science Source*; 16. Epub ahead of print 5 December 2017. DOI: 10.1186/s12940-017-0322-5.

[2] Jay O, Capon A, Berry P, et al. Reducing the health effects of hot weather and heat extremes: from personal cooling strategies to green cities. *The Lancet* 2021; 398: 709–724.

[3] Nazarian N, Lee JKW. Personal assessment of urban heat exposure: A systematic review. *Environmental Research Letters*; 16. Epub ahead of print 1 March 2021. DOI: 10.1088/1748-9326/abd350.

[4] Flouris AD, Dinas PC, Ioannou LG, et al. Workers' health and productivity under occupational heat strain: a systematic review and meta-analysis. *Lancet Planet Health* 2018; 2: e521–e531.

[5] Levi M, Kjellstrom T, Baldasseroni A. Impact of climate change on occupational health and productivity: A systematic literature review focusing on workplace heat. In: *Medicina del Lavoro*. Mattioli 1885, 2018, pp. 163–179.

[6] Ioannou LG, Foster J, Morris NB, et al. Occupational heat strain in outdoor workers: A comprehensive review and meta-analysis. *Temperature* 2022; 9: 67–102.

[7] Fiala D, Havenith G. Modelling Human Heat Transfer and Temperature Regulation. In: *Studies in Mechanobiology, Tissue Engineering and Biomaterials*. Springer, 2016, pp. 265–302.

[8] Hardin AW, Vanos JK. The influence of surface type on the absorbed radiation by a human under hot, dry conditions. *Int J Biometeorol* 2018; 62: 43–56.

[9] Vanos JK, Rykaczewski K, Middel A, et al. Improved methods for estimating mean radiant temperature in hot and sunny outdoor settings. DOI: 10.1007/s00484-021-02131-y/Published.

[10] Lim CL. Fundamental concepts of human thermoregulation and adaptation to heat: A review in the context of global warming. *Int J Environ Res Public Health* 2020; 17: 1–33.

[11] Islam MR, Golovin K, Dolez PI. Clothing Thermophysiological Comfort: A Textile Science Perspective. *Textiles* 2023; 3: 353–407.

[12] Scipioni M, Silva E, Farahi F. Solar absorption index (SAI) as a parameter to assess the coolness of fabrics exposed to sunlight. *Fibres & Textiles in Eastern Europe* 2020; 44–49.

[13] Rykaczewski K. Cool future fashion: Personal cooling as part of social adaptation to hotter climates. *Temperature*; 6. Epub ahead of print 2019. DOI: 10.1080/23328940.2019.1574201.

[14] Ichinose T, Pan Y, Yoshida Y. Clothing color effect as a target of the smallest scale climate change adaptation. *Int J Biometeorol* 2024; 68: 2029–2040.

[15] Tong JK, Huang X, Boriskina S V., et al. Infrared-Transparent Visible-Opaque Fabrics for Wearable Personal Thermal Management. *ACS Photonics* 2015; 2: 769–778.

[16] Peng Y, Cui Y. Advanced Textiles for Personal Thermal Management and Energy. *Joule* 2020; 4: 724–742.

[17] Chen M, Liu Y, Zhao X. Emerging passive thermoregulatory textiles through tailoring different heat transfer routes. *Textile Research Journal* 2023; 93: 3414–3439.
[18] Jiang S, Zhang K, Wang CF, et al. Recent advancements in radiative cooling textiles for personal thermal management. *Journal of Materials Chemistry A* 2024; 12: 14866–14884.
[19] Hasan KMF, Bai S, Chen S, et al. Nanotechnology-empowered radiative cooling and warming textiles. *Cell Rep Phys Sci*; 5.
[20] Zhu B, Li W, Zhang Q, et al. Subambient daytime radiative cooling textile based on nanoprocessed silk. *Nat Nanotechnol* 2021; 16: 1342–1348.
[21] Peng Y, Chen J, Song AY, et al. Nanoporous polyethylene microfibres for large-scale radiative cooling fabric. *Nat Sustain* 2018; 1: 105–112.
[22] Zhu F, Feng QQ. Recent advances in textile materials for personal radiative thermal management in indoor and outdoor environments. *International Journal of Thermal Sciences* 2021; 165: 106899.
[23] Tanaka M. Local skin thermal responses to heat radiation. 産業医学 1985; 27: 90–96.
[24] Kim T-K. Effects of Differents types of Clothing and Colours on Clothing Microclimate in the Subjects wearing Sports Wear under Sunlight. *The Korean Fashion and Textile Research Journal* 2001; 3: 271–276.
[25] Nielsen B. Solar heat load: heat balance during exercise in clothed subjects. *Eur J Appl Physiol Occup Physiol* 1990; 60: 452–456.
[26] Clark JA, Cena K. Net radiation and heat transfer through clothing: the effects of insulation and colour. *Ergonomics* 1978; 21: 691–696.
[27] Watanabe S, Koganezawa S, Horikoshi T, et al. Measurement of solar radiation absorptance of different clothing fabric for outdoor thermal comfort study. *Jpn J Biometeorol* 2008; 45: 121–129.
[28] Shimazaki Y, Goto S, Yoshida A, et al. The effect of solar radiation on temperature distribution in outdoor human–clothing–environment systems. *Int J Heat Mass Transf* 2017; 104: 1–6.
[29] Shimazaki Y, Yoshida A, Yamamoto T. Investigation of heat transfer and temperature distribution in outdoor human–clothing–environment systems with double-layered ensemble. *Int J Heat Mass Transf* 2017; 115: 523–529.
[30] Yuan J, Zhang C, Shimazaki Y, et al. Clothing Reflectance Effects on Mean Radiant Temperature and Outdoor Thermal Comfort under High Solar Radiation. *Case Studies in Thermal Engineering* 2026; 108290.
[31] Shimazaki Y, Tominaga N, Yuan J, et al. Passive cooling garments for outdoor thermal adaptation: a field experiment. *Int J Biometeorol* 2026; 70: 166.
[32] Ouyang S, Oh W, Gao S, et al. From black to radiative cooling: How fabric radiative properties shape outdoor thermal comfort and heat strain under extreme conditions. *Build Environ* 2026; 302: 114887.
[33] Zhou J, Zhao J, Guo X, et al. Personal Wearable Thermal and Moisture Management Clothing: A Review on Its Recent Trends and Performance Evaluation Methods. *Processes*; 11. Epub ahead of print 1 November 2023. DOI: 10.3390/pr11113063.
[34] Psikuta A, Allegrini J, Koelblen B, et al. Thermal manikins controlled by human thermoregulation models for energy efficiency and thermal comfort research–A review. *Renewable and Sustainable Energy Reviews* 2017; 78: 1315–1330.
[35] Bogerd N, Psikuta A, Daanen HAM, et al. How to measure thermal effects of personal cooling systems: human, thermal manikin and human simulator study. *Physiol Meas* 2010; 31: 1161.
[36] Hepokoski M, Curran A, Burke R, et al. *Simulating physiological response with a passive sensor manikin and an adaptive thermal manikin to predict thermal sensation and comfort*. SAE Technical Paper, 2015.
[37] Wang F. Physiological model controlled sweating thermal manikin: can it replace human subjects. *Journal of Ergonomics* 2011; 1: e103.
[38] Holmér I. Thermal manikin history and applications. *Eur J Appl Physiol* 2004; 92: 614–618.

[39] Zhou S, Yu Y, Kwok KCS, et al. Onsite measurements of pedestrian-level wind and preliminary assessment of effects of turbulence characteristics on human body convective heat transfer. *Energy Build* 2024; 114448.

[40] Danca PA, Nastase I, Croitoru C, et al. Thermal comfort evaluation inside a car parked under sun and shadow using a thermal manikin. In: *IOP Conference Series: Earth and Environmental Science*. IOP Publishing, 2021, p. 012064.

[41] Kuklane K, Gao C, Holmér I. Effects of natural solar radiation on manikin heat exchange. In: *3rd European Conference on Protective Clothing and NOKOBETEF 8. Protective clothing-towards balanced protection*. Central Institute for Labour Protection, Warszawa, Poland, 2006.

[42] Hu Z, Psikuta A, Rossi RM. Multi-sensor passive manikin—verification and potential applications for improving human safety, health, comfort and energy efficiency. *Results in Engineering* 2025; 108205.

[43] Hu Z, Psikuta A, Rossi RM. Strategies to characterize thermal exposure to convection-and radiation-based personal comfort systems: a comparative study. *Build Environ* 2025; 114088.

[44] Joshi A, Viswanathan SH, Jaiswal AK, et al. Characterization of human extreme heat exposure using an outdoor thermal manikin. *Science of the Total Environment* 2024; 923: 171525.

[45] Sadeghi K, Viswanathan SH, Joshi A, et al. Resolving shortwave and longwave irradiation distributions across the human body in outdoor built environments. *Build Environ* 2025; 277: 112934.

[46] Bogerd CP, Brühwiler PA. The role of head tilt, hair and wind speed on forced convective heat loss through full-face motorcycle helmets: a thermal manikin study. *Int J Ind Ergon* 2008; 38: 346–353.

[47] Bogerd CP, Rossi RM, Brühwiler PA. Thermal perception of ventilation changes in full-face motorcycle helmets: subject and manikin study. *Annals of occupational hygiene* 2011; 55: 192–201.

[48] Bogerd CP, Aerts J-M, Annaheim S, et al. A review on ergonomics of headgear: Thermal effects. *Int J Ind Ergon* 2015; 45: 1–12.

[49] Bröde P, Aerts J-M, De Bruyne G, et al. A modelling framework for local thermal comfort assessment related to bicycle helmet use. *J Therm Biol* 2023; 112: 103457.

[50] Pang TY, Subic A, Takla M. A comparative experimental study of the thermal properties of cricket helmets. *Int J Ind Ergon* 2013; 43: 161–169.

[51] Kim H-E, Park S-J. The effect of safety hat on thermal responses and working efficiency under a high temperature environment. *J Physiol Anthropol Appl Human Sci* 2004; 23: 149–153.

[52] Liu X, Abeysekera J, Shahnavaz H. Subjective evaluation of three helmets in cold laboratory and warm field conditions. *Int J Ind Ergon* 1999; 23: 223–230.

[53] Saleh A, Kanaan DA. An Experimental Study of a Novel System Used for Cooling the Protection Helmet. *Energies (Basel)* 2023; 16: 4046.

[54] Jun Y, Park CH, Shim H, et al. Thermal comfort properties of wearing caps from various textiles. *Textile Research Journal* 2009; 79: 179–189.

[55] Backes C, Religi A, Moccozet L, et al. Facial exposure to ultraviolet radiation: Predicted sun protection effectiveness of various hat styles. *Photodermatol Photoimmunol Photomed* 2018; 34: 330–337.

[56] Wimer GS. Wearing a cap, thermoregulation, and thermal sensation during running in a hot environment. *Journal of Sports Medicine and Physical Fitness* 2009; 49: 272.

[57] Jun Y, Park CH, Kang TJ. Effect of heat and moisture transfer properties on microclimate and subjective thermal comfort of caps. *Textile research journal* 2010; 80: 2195–2203.

[58] Middel A, Krayenhoff ES. Micrometeorological determinants of pedestrian thermal exposure during record-breaking heat in Tempe, Arizona: Introducing the MaRTy observational platform. *Science of the total environment* 2019; 687: 137–151.

[59] Joshi A, Bartels L, Viswanathan SH, et al. Evaluation of thermal properties and thermoregulatory impacts of lower back exosuit using thermal manikin. *Int J Ind Ergon* 2023; 98: 103517.

[60] De Dear RJ, Arens E, Hui Z, et al. Convective and radiative heat transfer coefficients for individual human body segments. *Int J Biometeorol* 1997; 40: 141–156.
[61] Ioannou LG, Tsoutsoubi L, Mantzios K, et al. The impacts of sun exposure on worker physiology and cognition: multi-country evidence and interventions. *Int J Environ Res Public Health* 2021; 18: 7698.
[62] Bergman TL, Lavine AS, Incropera FP, et al. *Fundamentals of heat and mass transfer*. New York: John Wiley & Sons, Inc, 2011.
[63] Lasisi T, Smallcombe J, Shriver MD, et al. Hair fiber morphology and function: at the intersection of anthropology, physiology, and engineering. *The FASEB Journal* 2020; 34: 1.
[64] Lasisi T, Smallcombe JW, Kenney WL, et al. Human scalp hair as a thermoregulatory adaptation. *Proceedings of the National Academy of Sciences* 2023; 120: e2301760120.

Funding

This research was supported by the National Science Foundation Leading Engineering for America's Prosperity, Health, and Infrastructure (LEAP HI) #2152468 award, while the thermal manikin was funded by a National Science Foundation Major Research Instrumentation grant #2117917. Joseph Rotella and Caitlyn Lyons were partially funded by Fulton Undergraduate Research Initiative scholarship.

Declaration of conflicts of interest/Competing interest

Authors have nothing to declare.

Ethics approval/declarations

Nothing to declare.

Consent to participate

Nothing to declare.

Consent for publication

Nothing to declare.

Author contributions

KR: conceptualization, experiments, analysis; JR, FA, SHV, CTJ, AP, CL: field experiments and analysis;

CTJ: optical property characterization;

All authors contributed to manuscript writing and editing;

All authors read and approved the final manuscript.

Availability of data and material/ Data availability

All data is included in the manuscript and supporting information.

Declaration of generative AI and AI-assisted technologies in the writing process

During the preparation of this work the author(s) used ChatGPT in order to improve the manuscript draft. After using this tool/service, the author(s) reviewed and edited the content as needed and take(s) full responsibility for the content of the publication.

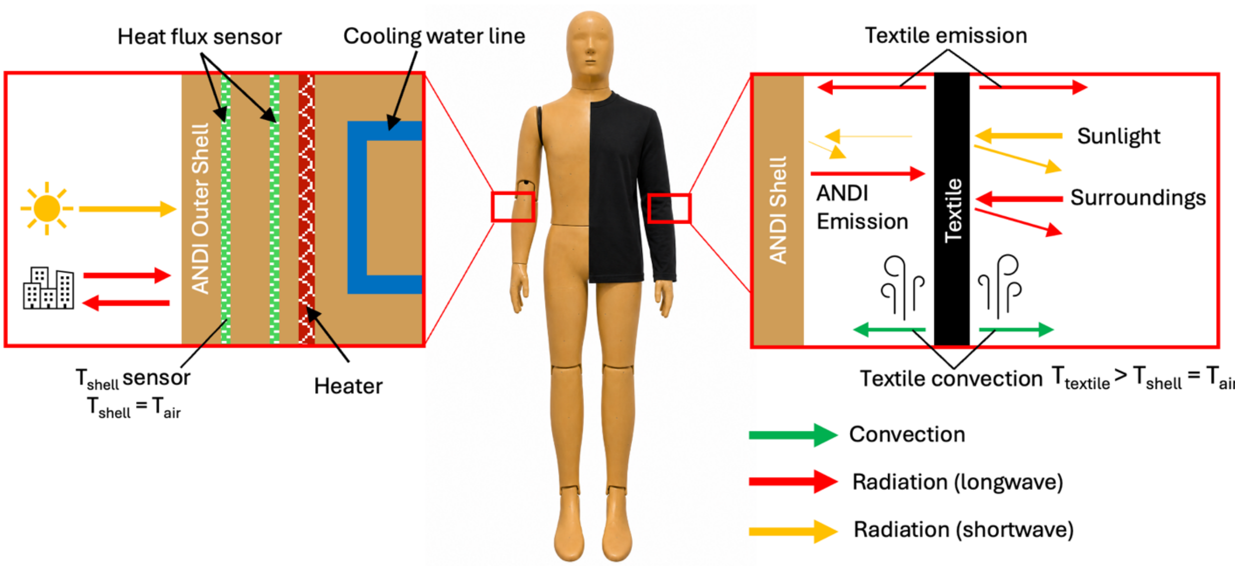

Fig.1. Schematic of the outdoor thermal ASU ANDI manikin showing schematically its internal sensors and heating/cooling abilities and what the net radiative heat flux measured by the manikin in "isothermal" experiments with shell temperature set to air temperature without (left) and with (right) a garment.

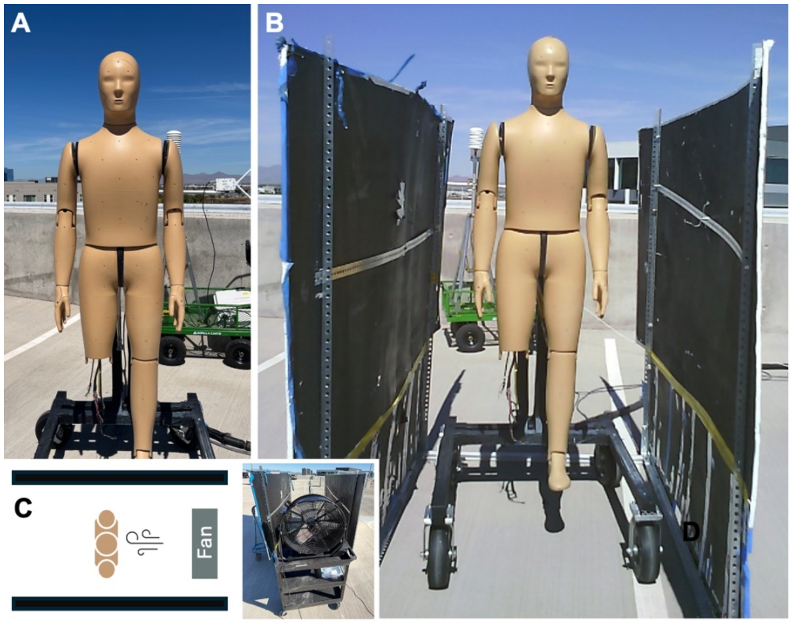

Fig.2. Images of thermal manikin measurement setups including **A.** fully exposed, B. in semi-wind tunnel without and **C.** with imposed fan.

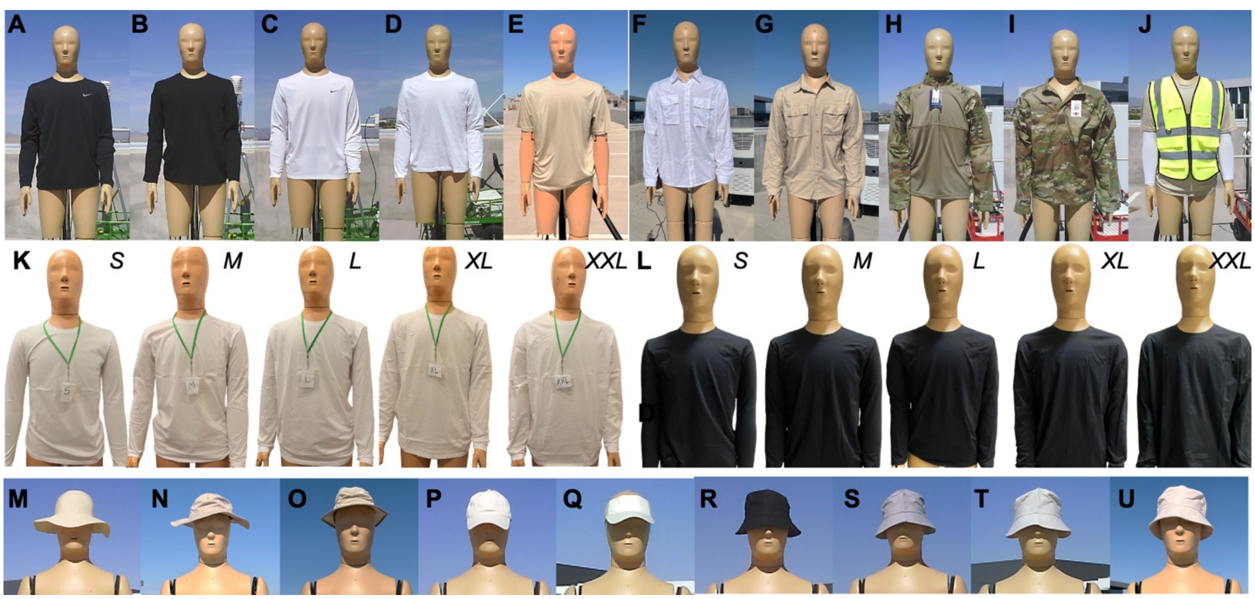

Fig.3. The shirts and hats tested in this study with specifics described in the text.

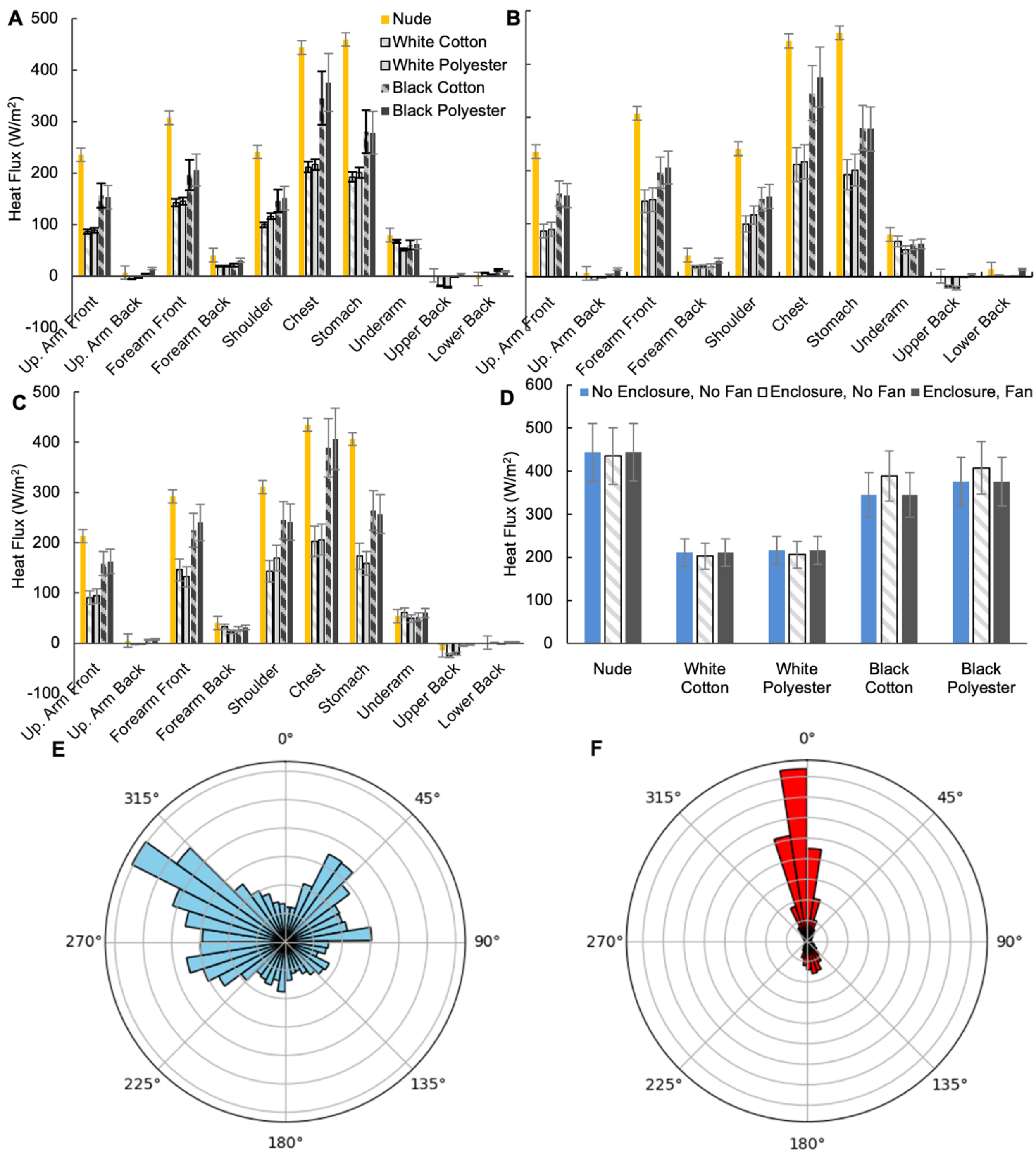

660

661 **Fig.4** Outdoor testing conducted with three different setups: **A.** ANDI standing without a fan or enclosure,
662 **B.** ANDI within the semi-outdoor wind tunnel with a fan, and **C.** ANDI with just the semi-outdoor wind
663 tunnel. **D.** shows a comparison of each testing condition for the manikin's chest zone. **E-F.** The wind
664 direction distribution **E.** outside the semi-outdoor wind tunnel (with 0° being North) and **F.** inside the tunnel
665 (very similar results were obtained with and without the fan being turned on). The error bars for clothing
666 measurements correspond to combined uncertainty of ±15% (80% confidence interval).

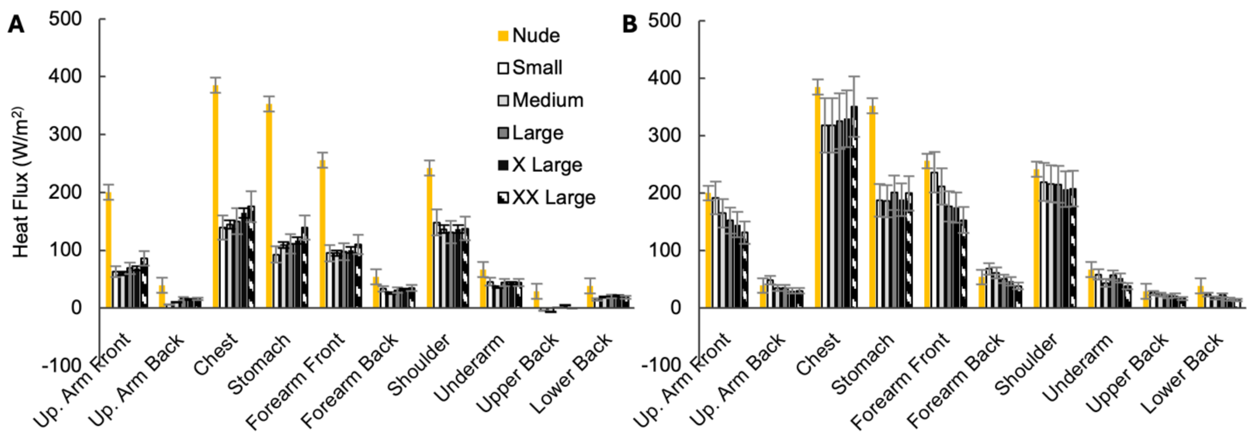

Fig. 5 Measured radiative net heat flux comparison across different shirt sizes for **A**. white and **B**. black long-sleeved shirts. The error bars for clothing measurements correspond to combined uncertainty of ±15% (80% confidence interval).

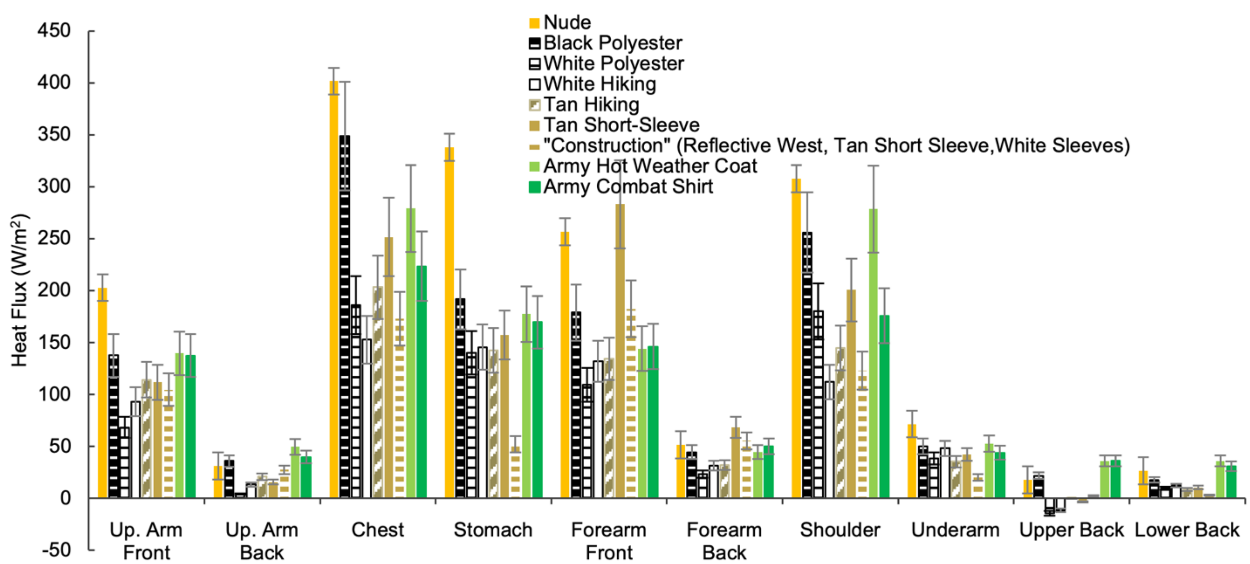

Fig. 6 Comparison of radiative net heat flux measured across upper body zones with a manikin wearing shirts with different styles and colors. The error bars for clothing measurements correspond to combined uncertainty of ±15% (80% confidence interval).

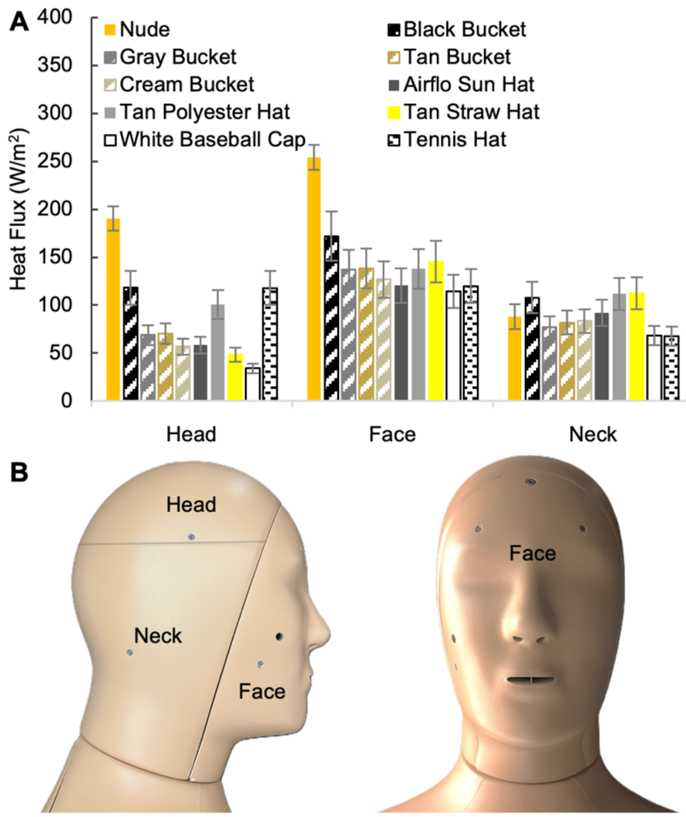

Fig. 7A. Comparison of radiative net heat flux measured across the head, face, and neck zones with a manikin wearing hats with assorted styles and colors; the error bars for clothing measurements correspond to combined uncertainty of ±15% (80% confidence interval). **B.** Images of the manikin showing the head, neck, and face zones.

Appendix 1

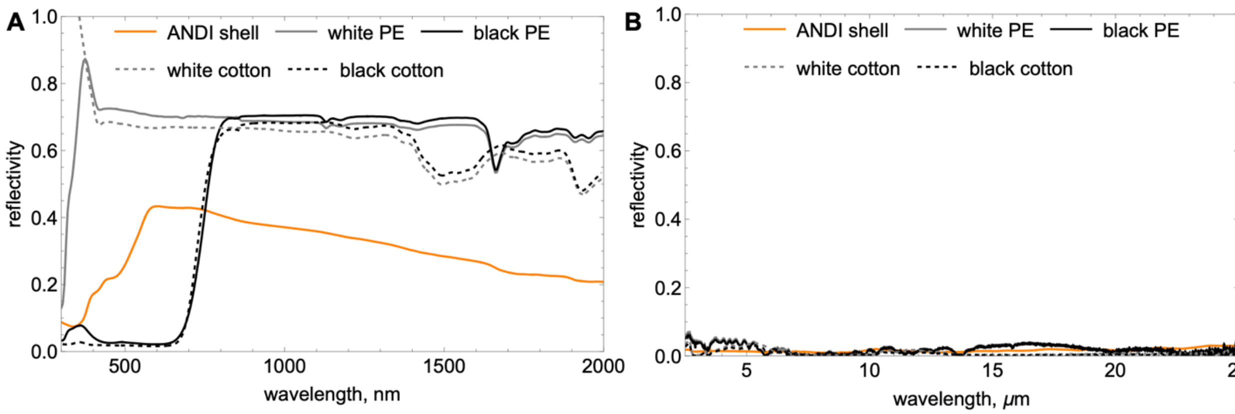

Fig. App1. The **A.** shortwave and **B.** longwave fractional spectral reflectance of black and white cotton and polyester (PE) shirts along with the manikin shell properties.